Published version: DOI [10.1109/TIM.2014.2365406]; https://ieeexplore.ieee.org/document/7001260?arnumber=7001260

Multiarea Distribution System State Estimation

Carlo Muscas, *Member, IEEE*, Marco Pau, *Student Member, IEEE*, Paolo Attilio Pegoraro, *Member, IEEE*, Sara Sulis, *Member, IEEE*, Ferdinanda Ponci, *Senior Member, IEEE* and Antonello Monti, *Senior Member, IEEE*

***Abstract*—This paper presents a new approach to the distribution system state estimation in wide-area networks. The main goal of the paper is to present a two step procedure designed to accurately estimate the status of a large scale distribution network, relying on a distributed measurement system in a multiarea framework. First of all, the network is divided into subareas, according to geographical and/or topological constraints and depending on the available measurement system. Then, in the first step of the estimation process, for each area, a dedicated estimator is used, exploiting all the measurement devices available on the field. In the second step, data provided by local estimators are further processed to refine the knowledge on the operating conditions of the network. To improve the accuracy of the estimation results, correlation arising in the first step estimations has to be suitably evaluated and considered during the second step. Performed analysis shows that existing correlations can be included in the estimation process with very low data exchange among areas, thus involving minimum communication costs. Both first and second steps can be performed in a decentralized way and with parallel processing, thus leading to reduced overall execution times. Test results, obtained on the 123-bus IEEE test network and proving the goodness of the proposed method, are presented and discussed.**

***Index Terms*—Correlation, decentralized architecture, distributed state estimation (SE), distribution system SE (DSSE), multiarea SE (MASE), phasor measurement unit (PMU), wide-area monitoring systems.**

I. Introduction

The distribution grid is the infrastructure used to transfer the electrical energy from the surroundings of inhabited areas, the limit of the transmission grid, to final customers. In modern power grids, such networks are operated through specifically designed distribution management systems (DMSs), which need an accurate knowledge of the network state to correctly apply active control [1]. Transmission systems have a redundant number of measurement devices and thus are generally fully observable. On the contrary, the distribution systems usually have a very limited number of measurement and monitoring devices, basically limited to high voltage/medium voltage (HV/MV) substations. As a consequence, monitoring of distribution networks requires estimators able to deal with nonredundant distributed measurement systems and to consider the peculiarities of such systems.

The so called distribution system state estimation (DSSE) is therefore a crucial module for each DMS application. The DSSE has to estimate the state of the network, in terms of node voltages or branch currents (BCs), starting from a few measurement data collected from heterogeneous instruments, which measure several electrical quantities with different accuracies and reporting rates. Thus, the ability to deal with several measurement sources in a fast way, leading to accurate estimations, is one of the main characteristics of a DSSE algorithm. This is crucial above all considering the new measurement devices. Recently, but only in some countries, power quality meters have been placed in the networks, mainly on the HV/MV substations. In addition, the development of a new generation of electronic measurement systems, measuring different quantities, and able to communicate with control centers, has encouraged new research activities on state estimation (SE) [2]–[4]. In particular, it is possible to mention the phasor measurement units (PMUs), measuring synchrophasors at high reporting rate with really high accuracy. It is therefore clear that DSSE is a complex measurement methodology, whose characterization in terms of accuracy of the measurement results is decisive for downstream decisions. It is worth noting that an incorrect evaluation of the accuracy of the DSSE results has a significant impact on all the advanced procedures that are based on these data. The crucial role of DMS actions based on DSSE results in operating distribution systems is a prime example of the sensitivity of this issue.

Several DSSE techniques, mostly based on a weighted least squares (WLSs) formulation, have been presented in literature (see, for instance, [5]–[9]). Each of them focuses on specific characteristics of the estimation method and of the distribution networks. To achieve an accurate knowledge of the network state, due attention must be paid to the proper modeling of the estimation problem. A detailed description of the measurement model is needed [10] and possible correlation existing in the measurements should be duly considered [11].

A particularly important problem for distribution networks is that, due to the large number of nodes and to the possibly unbalanced three-phase structure, long calculation times, and large data storage requirements can be required. Multiarea SE (MASE) methods address this issue [12]. However, in the literature, only a few works deal with the problem of MASE applied to distribution systems. In [13], an MASE approach based on a differential evolution algorithm is proposed. The network state is obtained using local estimators that need to exchange information with the adjacent subareas at each iteration of the estimation algorithm. In [14], a method based on local WLS estimators is presented. The voltage profile of the whole network is obtained in a second step through a central coordinator, which exploits the results of the local estimations.

In [15], a study on different MASE approaches, critically analyzed and tested for applicability in distribution systems, is

C. Muscas, M. Pau, P. A. Pegoraro, S. Sulis are with the Department of Electrical and Electronic Engineering of the University of Cagliari, Piazza d'Armi, 09123 Cagliari, Italy (email: [carlo, marco.pau, paolo.pegoraro, sara.sulis]@diee.unica.it).

F. Ponci and A. Monti are with the Institute for Automation of Complex Power Systems of the E.ON Energy Research Center at RWTH Aachen University, Aachen, Germany (e-mail: [fponci, amonti]@eonerc.rwth-aachen.de).

proposed. For all the considered cases, the DSSE problem is split into independent estimators working in parallel on local subnetworks; then, their outputs are coordinated to improve the whole wide-area estimation. The need to exchange information between subareas is inherently met in the case of a single distribution system operator (DSO) managing all the subnetworks. However, in a future scenario the roles of the DSOs are expected to change, so data exchange with external entities (e.g. aggregators) can be foreseen, possibly regulated or enforced by a supervisory authority. For this reason, the proposed multiarea approach is designed for minimum data exchange among the adjacent subareas, which supports applicability even in a competitive scenario. Starting from the results shown in [15], in this paper, a new approach for a two-step procedure for an accurate decentralized DSSE is presented. One crucial point in this approach is that different sub-areas need to share measurement devices to guarantee accurate estimation in most conditions. This requirement depends on the scarcity of measurement devices with respect to the number of the quantities to be estimated. At least one measurement device is necessary in each area, so that, even in case of communication problems, a sufficiently accurate estimation could be obtained. Sharing measurement devices among different areas leads to the presence of correlations among the local estimations. To properly refine the estimation results, existing correlations have to be suitably evaluated and considered in the estimation process. In this paper, the assessment of such correlations has been performed and the benefits coming from their use in the multiarea approach are shown. In the following, the fundamentals of the method are presented and the most significant results, obtained on the 123-bus IEEE distribution network, are presented and discussed. This test network is a standard passive distribution grid, and it has been chosen because it represents a common IEEE benchmark for this kind of studies. However, there is no conceptual limitation in applying the approach to active distribution systems.

II. Distribution System State Estimation

SE methods are complex measurement methodologies that evaluate the state of grids from heterogeneous sets of measurements. SE techniques, developed and used for transmission systems, cannot be directly applied to distribution grids, due to their peculiarities. To mention some of them, the number of nodes is very large with respect to the real-time measurements, and information on the behavior of the loads can be really limited. For this reason, any kind of available a priori information has to be used to make the system observable. This prior information, which is necessary but also highly uncertain because it is obtained above all from historical data of the power drawn by the loads, is commonly referred to as pseudomeasurements.

The general measurement model used for SE problem is:

$$\mathbf{z} = \mathbf{h}(\mathbf{x}) + \mathbf{e} \tag{1}$$

where $\mathbf{z} = [z_1 \dots z_M]^{\mathrm{T}}$ is the vector of the M measurements of the network (including the chosen pseudo-measurements); $\mathbf{h} = [h_1 \dots h_M]^{\mathrm{T}}$ is the vector of measurement functions, in general nonlinear (depending on the type of measurements and on the network topology, which is assumed to be known); $\mathbf{x} = [x_1 \dots x_N]^{\mathrm{T}}$ is the vector of the N state variables; and $\mathbf{e}$ is the measurement noise vector, assumed to be zero mean and Gaussian, with known covariance matrix $\Sigma_{\mathbf{z}}$. Starting from this measurement model, different estimation algorithms can be derived.

In this paper, the three-phase version of the efficient BC-DSSE presented in [9] is used, since it allows for easy integration of any kind of electrical measurement. According to [9], the state vector $\mathbf{x}$ includes the reference (or slack) bus voltage, as well as the currents in the N_{br} branches, in rectangular coordinates. The state $\mathbf{x}$ is thus $\left[V_{slack}, i_1^r \dots i_{N_{\mathrm{br}}}^r, i_1^x \dots i_{N_{\mathrm{br}}}^x\right]^{\mathrm{T}}$ (where $V_{slack} \triangleq |v_{slack}|$ is the absolute value of the complex slack bus voltage) if the measurement system is composed of only traditional measurements (voltage and current magnitudes, active and reactive powers and power injections), whereas $\mathbf{x}$ is $\left[v_{slack}^r, v_{slack}^x, i_1^r \dots i_{N_{\mathrm{br}}}^r, i_1^x \dots i_{N_{\mathrm{br}}}^x\right]^{\mathrm{T}}$ if the synchrophasor measurements (voltage and current provided by PMUs) are also available.

The branch currents are estimated iteratively by means of WLS step and forward sweep step (see [9] for further details).

In the WLS step, the equations are solved as follows:

$$\Delta\mathbf{x}_n = \mathbf{x}_{n+1} - \mathbf{x}_n = \mathbf{G}_n^{-1}\mathbf{H}_n^{\mathrm{T}}\mathbf{W}\Delta\mathbf{z}_n \tag{2}$$

where $\mathbf{x_n}$ is the state vector at iteration n; $\mathbf{\Delta z}_n = [\mathbf{z} - \mathbf{h}(\mathbf{x}_n)]$ is the vector of the measurement residuals; $\mathbf{H}_n$ is the Jacobian of the measurement functions with respect to the state variables; $\mathbf{W}$ is the weighting matrix, usually chosen as the inverse of the measurement error covariance matrix $\Sigma_{\mathbf{z}}$; $\mathbf{G}_n = \mathbf{H}^{\mathrm{T}}\mathbf{W}\mathbf{H}$ is the so-called Gain matrix and its inverse corresponds to the covariance matrix of the estimated vector (see [16] for details).

A forward sweep step is then performed at each iteration to compute, starting from the estimated branch currents, the network voltages for each node.

III. Multi-Area Distribution System State Estimation

MASE methods address the problem of performing SE on wide-area systems. The major aims are to exploit the characteristics of the computational nodes distributed over the grid and to reduce the computing time [12]. MASE methods can be categorized according to the methodology adopted to define the subareas, the type of estimator, and the harmonization process carried out in the estimator [12]–[14], [17]–[20]. MASE methods, in general developed for transmission systems, have to be designed in a different way to be suitable for the features of the distribution grids. In the following, the proposed procedure is presented.

A. Definition of the Subareas

In Fig. 1 a sketch of the distributed measurement system organization for multiarea DSSE is shown. The proposed solution is based on the following assumptions.

- The division into areas can be based on topological or geographical criteria but, in general, it should be handled

so that areas have similar number of nodes, to minimize the execution time of the individual DSSE.
- Adjacent areas are overlapped and share at least one node; this node is fully monitored through a suitable measurement point and can be shared by more than two subareas.
- Each measurement point includes a voltage measurement and as many flow measurements (power or current) as the branches converging to the node of interest.
- Each area has a mini-control center where the local estimation is carried out; such computing nodes work in parallel and communicate with the intelligent nodes of adjacent areas.

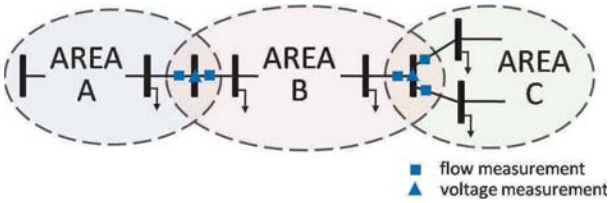

Fig. 1. Multiarea network division schema.

The proposed solution with overlapping nodes has different advantages. First of all, if the pseudomeasurements of power injection on the nodes are available, observability and at least one measurement point are guaranteed in each area. This is crucial for robustness to communication failure. In addition, measurements on the branches connected to the shared node, but not belonging to the area of interest, can be used to obtain the equivalent power injection of the adjacent subaeras, thus increasing the measurement redundancy in the area itself. Finally, in case of traditional measurements, the phase angles of each area can be simply sequentially shifted, starting from the area with the absolute phase-angle reference, using the difference in the phase-angle estimation on the overlapped nodes, to achieve consistent angle information on the whole network.

The same kind of architecture has been used in [15], where the two-step procedure was introduced. In the first step, the estimation is performed locally, in each area, by means of BC-DSSE; in the second step, the results provided by the previous step are harmonized to obtain a more accurate estimation. This second step can be implemented in different ways: three possibilities were analyzed in [15]. In this paper, a new solution (MA-DSSE henceforth) is proposed, which is an enhancement of method 3 in [15].

B. Proposed Multiarea DSSE Approach

In the following, the bases of the proposed MA-DSSE approach are described. In particular, the estimated quantities are indicated with the hat symbol. The algorithm operates as follows.

1) First Step: All the measurements internal to the considered area are exploited to perform a local estimation. Moreover, flow measurements on the branches converging to each shared node, but external to the considered area, are used as equivalent injection measurements. The BC-DSSE for all the areas is performed in parallel and in a totally independent manner, obtaining for each area i the estimated state $\hat{\mathbf{x}}_i$. Each area must be ready to provide, in addition to the values of the estimates, their corresponding variances.

2) Second Step: A second SE is performed on each area using as measurements the results of the previous estimation and the estimates of the border quantities provided by adjacent areas. For each area i, defining as Γ_i the set of adjacent areas and v_s the voltage of the generic shared node between two areas i and j, the following data inputs are used.
- The output $\hat{\mathbf{x}}_i$ of the first step estimation in the considered area i.
- For each area $j \in \Gamma_i$, the estimate of the shared node voltage from area j and the estimates of the currents in the branches connecting the shared node to the rest of area j (lumped up to a single equivalent current injection for area i).

If only traditional measurements are used, the estimated absolute value $\hat{V}_{s_j} = |\hat{v}_{s_j}|$ of the shared node is considered. For the currents, a realignment of their phase angle is performed (exploiting the mismatch of the phase-angle estimation on the shared node) to refer them to the same reference phase angle of area i. Instead, if PMU measurements are present, the absolute phase angles can be estimated in all the areas and then the voltages $\hat{v}_{s_j}$ in rectangular coordinates contribute to the refinement of the phase-angle estimation. In addition, no alignment process is needed for the currents.

The second step is therefore implemented by another BC-DSSE applied to the following equivalent measurement model (referred to a generic area i):

$$\mathbf{y} = \begin{bmatrix} \hat{\mathbf{x}}_i \\ \mathbf{y}_j \\ \vdots \end{bmatrix} = \begin{bmatrix} \mathbf{x}_i \\ \mathbf{f}_j(\mathbf{x}_i) \\ \vdots \end{bmatrix} + \begin{bmatrix} \boldsymbol{\epsilon}_i \\ \boldsymbol{\eta}_j \\ \vdots \end{bmatrix} \tag{3}$$

where $\mathbf{y}$ is the vector of second step measurements, $\mathbf{y}_j$ is the vector of the estimates coming from area j, $\mathbf{f}_j(\mathbf{x}_i)$ is the vector of the measurement functions linking the estimates from area j to the state of area i, and $\boldsymbol{\epsilon}_i$ and $\boldsymbol{\eta}_j$ are, respectively, the vectors of estimation errors in the first step, in area i and area j (limited to the border quantities of interest). Similarly to the first step, these errors can be modeled through a covariance matrix $\Sigma_{\mathbf{y}}$ and its inverse should be considered as weighting matrix for the second step.

In method 3 of [15], the matrix $\Sigma_{\mathbf{y}}$ was built, in a first approximation, using the variances of all the estimated quantities involved in (3), obtained at the end of the first step, whereas the correlation was not considered. However, correlation in the measurement process exists because the measurements on the overlapped nodes are shared by different zones. For this reason, in this paper, an analysis of such correlations has been performed. Section IV describes the calculation of the covariance terms to be included in $\Sigma_{\mathbf{y}}$ in the second step of the estimation. This calculation does not require the communication of additional data between areas i and j.

IV. Correlation among States Estimated in Different Areas

This section reports the analysis of the correlation among the states estimated in the first step with shared available

measurements. To formalize this correlation, it is necessary to relate the state estimates with the measurements.

Considering only the last iteration of the estimation algorithm and with the linearized measurement functions (2), the solution yields:

$$\Delta\hat{\mathbf{x}} = \mathbf{B}\Delta\mathbf{z} \tag{4}$$

where $\mathbf{B} = (\mathbf{H}^{\mathrm{T}}\mathbf{W}\mathbf{H})^{-1}\mathbf{H}^{\mathrm{T}}\mathbf{W}$ is the pseudoinverse matrix linking the estimated states to the measurement residuals.

Two generic areas A and B, characterized by N_i states and M_i measurements, (with $i = [A, B]$), have an $[N_i \times 1]$ state vector $\mathbf{x}_i$ and an $[M_i \times 1]$ measurement vector $\mathbf{z}_i$. Hence, each area has an $[M_i \times N_i]$ Jacobian matrix $\mathbf{H}_i$ and an $[M_i \times M_i]$ weighting matrix $\mathbf{W}_i$.

If the measurements shared between the two areas are M_{AB}, then the total number of measurements available in the two areas is: $M = M_A + M_B - M_{AB}$. It is possible to create a $[M \times 1]$ measurement vector $\mathbf{z}_{TOT}$ and a $[M \times M]$ weighting matrix $\mathbf{W}_{TOT}$ including all the available measurements. For each area, it is also possible to create an expanded Jacobian matrix $\mathbf{H}_{i_{TOT}}$ involving the relationship among all the measurements of the network and the state of the area: in this case, all the measurements not belonging to the considered area will have null elements in the corresponding rows of the Jacobian.

Let us define the measurement vector $\mathbf{z}_{TOT}$ as follows:

$$\mathbf{z}_{TOT} = \begin{bmatrix} \mathbf{z}_{AA} \\ \mathbf{z}_{AB} \\ \mathbf{z}_{BB} \end{bmatrix} \tag{5}$$

where $\mathbf{z}_{AA}$ is the subvector of the M_{AA} measurements belonging only to area A, $\mathbf{z}_{BB}$ is the subvector of the M_{BB} measurements belonging only to area B, and $\mathbf{z}_{AB}$ is the subvector of the M_{AB} measurements shared between the two areas. Then the expanded Jacobians for the two areas are:

$$\mathbf{H}_{A_{TOT}} = \begin{bmatrix} \mathbf{H}_A \\ \mathbf{0} \end{bmatrix}, \ \mathbf{H}_{B_{TOT}} = \begin{bmatrix} \mathbf{0} \\ \mathbf{H}_B \end{bmatrix} \tag{6}$$

According to the construction of the measurement vector, the overall weighting matrix can be expressed as:

$$\mathbf{W}_{TOT} = \begin{bmatrix} \mathbf{W}_{AA} & \mathbf{0} & \mathbf{0} \\ \mathbf{0} & \mathbf{W}_{AB} & \mathbf{0} \\ \mathbf{0} & \mathbf{0} & \mathbf{W}_{BB} \end{bmatrix} \tag{7}$$

where $\mathbf{W}_{AA}$, $\mathbf{W}_{AB}$, and $\mathbf{W}_{BB}$ are the diagonal submatrices composed of the weights associated to the M_{AA}, M_{AB}, and M_{BB} measurements (considered as uncorrelated), respectively.

Considering the gain matrix of area i:

$$\mathbf{G}_i = \mathbf{H}_i^{\mathrm{T}}\mathbf{W}_i\mathbf{H}_i \tag{8}$$

the following relationship holds:

$$\mathbf{G}_i = \mathbf{H}_{i_{TOT}}^{T}\mathbf{W}_{TOT}\mathbf{H}_{i_{TOT}} \tag{9}$$

Since the inverse of each area gain matrix gives the covariance matrix $\mathbf{\Sigma}_i = \mathbf{G}_i^{-1}$ of the state estimated in the first step of the multiarea procedure for the corresponding area, from (9) it follows that:

$$\mathbf{B}_{i_{TOT}} = \mathbf{\Sigma}_i\mathbf{H}_{i_{TOT}}^{T}\mathbf{W}_{TOT} \tag{10}$$

where $\mathbf{B}_{i_{TOT}}$ is the matrix linking the estimates of area i to the measurement vector $\mathbf{z}_{TOT}$.

Considering (6) for the Jacobian matrices and (7) for the overall weighting matrix, the following two matrices can be defined:

$$\mathbf{B}_{A_{TOT}} = \begin{bmatrix} \mathbf{B}_A & \mathbf{0} \end{bmatrix}, \ \mathbf{B}_{B_{TOT}} = \begin{bmatrix} \mathbf{0} & \mathbf{B}_B \end{bmatrix} \tag{11}$$

where $\mathbf{B}_A$ and $\mathbf{B}_B$ are, respectively:

$$\mathbf{B}_A = \mathbf{\Sigma}_A\mathbf{H}_A^{\mathrm{T}}\mathbf{W}_A, \ \ \mathbf{B}_B = \mathbf{\Sigma}_B\mathbf{H}_B^{\mathrm{T}}\mathbf{W}_B \tag{12}$$

The covariances $\mathbf{\Sigma}_{\hat{\mathbf{x}}_A,\hat{\mathbf{x}}_B}$ among the estimated states of areas A and B can thus be found as follows:

$$\mathbf{\Sigma}_{\hat{\mathbf{x}}_A,\hat{\mathbf{x}}_B} = \mathbf{B}_{A_{TOT}}\mathbf{\Sigma}_{\mathbf{z}_{TOT}}\mathbf{B}_{B_{TOT}}^{\mathrm{T}} \tag{13}$$

where $\mathbf{\Sigma}_{\mathbf{z}_{TOT}}$ is the covariance matrix of all the measurement errors. Considering that the weighting matrix is chosen as the inverse of the measurement error covariance matrix, (13) becomes:

$$\mathbf{\Sigma}_{\hat{\mathbf{x}}_A,\hat{\mathbf{x}}_B} = \mathbf{B}_{A_{TOT}}\mathbf{W}_{TOT}^{-1}\mathbf{B}_{B_{TOT}}^{\mathrm{T}} \tag{14}$$

and using (11), after some simplifications (mathematical details can be found in Appendix A) it is possible to obtain the following expression for the covariance matrix:

$$\mathbf{\Sigma}_{\hat{\mathbf{x}}_A,\hat{\mathbf{x}}_B} = \mathbf{\Sigma}_A\mathbf{H}_{AB}^{\mathrm{T}}\mathbf{W}_{AB}\mathbf{H}_{BA}\mathbf{\Sigma}_B \tag{15}$$

where $\mathbf{H}_{AB}$, $\mathbf{H}_{BB}$, $\mathbf{H}_{BA}$, and $\mathbf{H}_{BB}$ are matrices obtained by splitting (in the Jacobians) the contribution of the shared measurements and of the measurements that are exclusively pertaining to each area (Appendix A).

In the following sections more details are given for the covariance computation in case that either traditional or synchronized measurements are used.

A. Covariance Among Voltages Estimated in Different Areas With Traditional Measurements

Equation (15) provides the covariances existing among all the state variables estimated in areas A and B. However, it is worth highlighting that in the case of interest for this paper, the searched covariance is limited to that between the voltage magnitudes of the overlapping node estimated in the two subareas.

According to [9], as briefly recollected in Section II, the state vector of a branch-current estimator is composed by the currents of all the branches and the voltage in the slack bus. Since the uncertainty of the estimation does not depend on the choice of the slack bus (in [21], the possibility to avoid a reference bus without drawbacks in the estimation is discussed for transmission systems), in the following, for presentation simplicity, the overlapping node is chosen as the reference bus for both the areas.

In particular, if only traditional measurements are present, only the voltage amplitude at the shared node has to be considered. Thus, assuming the organisation of the state is the same for both states $\mathbf{x}_A$ and $\mathbf{x}_B$, with the voltage magnitude of the shared node at index 1, only the element $(1, 1)$ of $\mathbf{\Sigma}_{\hat{\mathbf{x}}_A,\hat{\mathbf{x}}_B}$ has to be computed. Such element is obtained considering only the first row of $\mathbf{\Sigma}_A$ and the first column of $\mathbf{\Sigma}_B$ in

(15). Furthermore, it is $\mathbf{H}_{AB} = \mathbf{H}_{BA} = [1, 0, \ldots, 0]$ and $\mathbf{W}_{AB} = w_{z_{V_s}}$, where $w_{z_{V_s}} = 1/\sigma^2_{z_{V_s}}$ is the weight associated to the measurement z_{V_s} (with variance $\sigma^2_{z_{V_s}}$) of the voltage magnitude in the overlapped node. The only contribution to the sought covariance of the first estimation step is given by the variances of the estimated overlapping node voltages. The resulting covariance term is therefore:

$$\sigma_{V_{s_A}, V_{s_B}} = \sigma^2_{V_{s_A}} w_{z_{V_s}} \sigma^2_{V_{s_B}} \tag{16}$$

where $\sigma^2_{V_{s_i}}$ is the variance of the overlapping node voltage estimated in the area i.

B. Covariance Among Voltages Estimated in Different Areas With Phasor Measurements

When PMU measurements are used, many of the aforementioned considerations for the case of traditional measurements still hold. The main difference with respect to the previous case is that the reference node voltage included into the state vector is given in terms of real and imaginary parts. As a consequence, there are two shared measurements between areas A and B, which are the real and the imaginary parts of the voltage phasor measurement in the overlapping node.

According to these assumptions, it is possible to compute the correlation matrix from (15), considering that H_{AB} and H_{BA} have two rows. Four correlation terms have to be included in the second step of the multiarea estimator needed in this case, because of the two state variables that are common to both areas, and it is possible to show that it can be obtained with a simple generalization of (16) to two variables. The mathematical passages are detailed in Appendix B.

V. Tests and results

The unbalanced IEEE 123-bus network is considered as test system. Data about the network were obtained from [22]. Fig. 2 shows the grid topology and the chosen decomposition in overlapping areas. Several tests have been performed, with different measurement systems, to establish the accuracy performance of the proposed method. In the following, the most significant results in terms of root mean square errors (RMSEs) of the node voltage magnitude and phase-angle estimations are presented and discussed.

According to the proposed method, a measurement point is considered in each one of the resulting shared nodes (18 and 67) to guarantee the local area observability. In addition, a measurement point in the primary station (node 150) has been considered. The starting measurement configuration is thus composed by measurement devices on the nodes 18, 67, and 150. Each one of the measurement points includes a voltage magnitude measurement on the node and power measurements on all the branches connected to it. The alternative of having PMU measurements has been also considered. In this case, the available measurements are the voltage phasor on the node and the current phasors on the branches. In addition to the real measurements, pseudomeasurements of the power injections on all the nodes are supposed to be known.

To evaluate the accuracy performance of the proposed MA-DSSE method, several tests have been performed using Monte Carlo (MC) simulations. At the beginning, true values of the electrical quantities in the network are obtained by means of a load flow calculation. Then, starting from such reference values, for each MC trial, measurements are randomly extracted according to their probability density function. In particular, the following assumptions have been considered.

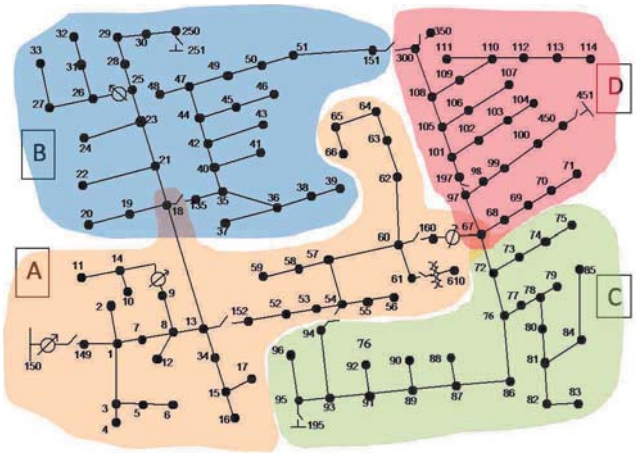

Fig. 2. IEEE 123-bus test network

- Number of MC trials $N_{MC} = 50000$.
- Pseudomeasurements of node power injection with Gaussian distribution and $3\sigma = 50\,\%$ of the nominal value.
- Real measurements with Gaussian distribution and 3σ equal to accuracy values. As for the traditional measurements, accuracy equal to $1\,\%$ and $3\,\%$ are used for voltage magnitude and power flow measurements, respectively. In case of PMU measurements, accuracy of $0.7\,\%$ and 0.7 crad ($0.7 \cdot 10^{-2}$ rad) is considered for magnitude and phase-angle measurements, respectively.

To assess the performance of the proposed MA-DSSE method, its results have been compared with those obtained with the BC-DSSE carried out on the whole network [integrated SE, (ISE)], the first step estimation on the different areas [local SE, (LSE)] and the method 1 of [15], indicated as MASE 1 in the following. MASE 1 compares voltage estimations at the shared nodes, as calculated by the estimators of the overlapping areas and uses the most accurate estimate to correct the voltage profiles on the zones with worse estimates.

In the first test series, the starting measurement configuration has been considered. First of all, the validity of the mathematical approach developed for computing the covariances to be used in the second step of the MA-DSSE has been checked. Table I shows the comparison between the correlation factors evaluated according to Section IV and the ones obtained by means of the MC simulations. Results show that there is a good match between the correlation factors, confirming the validity of the found relationships. It is also worth noting that, depending on the measurement configuration, there could be situations in which two estimations are fully correlated (in this example, the estimations coming from areas C and D): in this case, only one of them is included in the second step.

Fig. 3 shows the results, in terms of RMSE, obtained for the voltage magnitude estimation in case of voltage and power

TABLE I
CORRELATION BETWEEN ESTIMATED VOLTAGES

Voltage estimations	Theoretical calculation	Monte Carlo calculation
V_{150}^{A} - V_{18}^{B}	0.581	0.581
V_{150}^{A} - V_{67}^{C}	0.585	0.583
V_{150}^{A} - V_{67}^{D}	0.585	0.583
V_{67}^{C} - V_{67}^{D}	1.000	1.000

measurements. Here and in the following, results refer to only one phase of the system, but equivalent results and the same considerations were found to hold for all the three phases. The node numeration of Fig. 3 does not match the one of Fig. 2 because the nodes have been renumbered to aggregate the results related to same areas. Moreover, the shown nodes are only 80 because several of the laterals are single-phase branches. To avoid a complex representation, each node is reported only once and the shared nodes are represented only in area A section of the figure. For LSEs and MASE methods, the shared nodes' voltages present, for each area, RMSEs that are similar to those of the other nodes, as can be deduced by the flatness of the profile. As an example, the RMSE of LSE in node 18 is $0.199\,\%$ for area A while it is $0.333\,\%$ for area B. Similar considerations hold for the following tests.

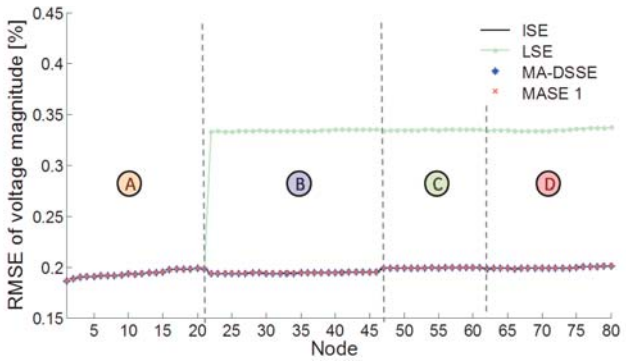

Fig. 3. RMSE of voltage magnitude estimation with starting measurement configuration

An important aspect is highlighted by the LSE results. In case of area A, the LSE has accuracy performance equal to the ISE: this is an expected result because area A includes all the measurements available on the network. In the other areas, instead, the LSEs have significantly less accurate estimations with respect to the ISE, since LSEs can rely only on one measurement point. This underlines the importance of using suitable two-step techniques to improve the local estimations.

As for the multi-area approaches, both MA-DSSE and MASE 1 exhibit the same accuracy of ISE in all the areas. In MA-DSSE, the reason is that the second step allows integrating in the estimation the information coming from the voltage estimated in the adjacent areas. In particular, areas B, C, and D can exploit the accurate estimation coming from area A to achieve a better estimation. It is important to highlight that such accuracy results can be obtained only through a proper modeling of the correlations among the voltages used in the second step. In [15], where covariances were not included in the second step of this approach, in the same test conditions, the proposed method provided worse results than the ISE in all the areas. As for MASE 1, instead, the voltage correction performed in the second step leads to propagate the best accuracy of area A also to the adjacent areas. Thus, since the first step estimation in area A is similar to the ISE, this similarity is also propagated to the other areas. Analogous results have been found also in case of PMU measurements.

Different considerations apply to the voltage phase-angle estimation. In this case, a distinction between the use of traditional and phasor measurements is needed. Indeed, using traditional measurements, the voltage phase angles are computed as phase-angle differences with respect to a chosen reference bus; instead, when PMUs are available, absolute phase angles with respect to the coordinated universal time (UTC) reference can be estimated. In case of traditional measurements, to assume node 150 as universal slack bus (and to allow comparison with the ISE results) an alignment of the phase angles is needed, using the phase-angle mismatch at the shared nodes. Results show that all the estimators provide very similar results, with RMSEs largely lower than 1 mrad in all the nodes. In case of PMU measurements, the alignment step is not needed, since all the phase-angle estimations already refer to the UTC. The RMSEs, in this case, show the same trend as shown in Fig. 3 for the voltage magnitude, with lower accuracies for the LSEs of areas B, C, and D (the mean RMSE obtained averaging among the nodes is 2.3 mrad in each area) and similar accuracies for the ISE and the multiarea methods (with a mean RMSE of 1.4 mrad in all the areas). It is worth to highlight that if, starting from the absolute phase angles, the phase-angle differences with respect to a reference node are calculated, even in this case the achievable RMSEs are largely lower than 1 mrad.

This first test shows that the MA-DSSE (but also the MASE 1 method) is able to achieve accuracy performance similar to the ISE, for both voltage magnitude and phase-angle estimation, when there is an area including all the available measurements and all the other areas are adjacent to this one. Different results can be instead expected when differing measurement scenarios are assumed.

As an example, a second test has been performed adding a measurement point at nodes 86 (area C) and 105 (area D). Fig. 4 shows the RMSEs obtained for the voltage magnitude estimation in case of traditional measurements.

In this case, obviously, the ISE provides the best estimation results, since it can simultaneously process all the available measurements. As in the previous test, instead, the LSE results are significantly less accurate. In particular, it is possible to observe that the achieved estimation accuracy is strictly related to the number of voltage measurements available in each area: thus, area A provides the best results, since it can rely on three voltage measurements, while area B, having only one voltage measurement, gives the worst estimation.

Looking at the multiarea approaches, both of them allow to improve the accuracy of the LSE. However, in this measurement scenario, the advantages coming from the use of the MA-DSSE become evident. MASE 1 exploits the best local

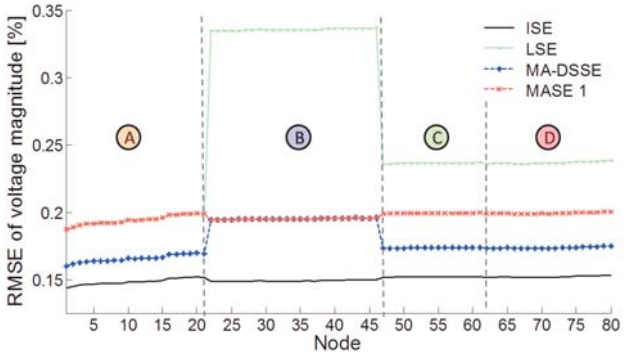

Fig. 4. RMSE of voltage magnitude estimation with additional measurement points

estimation of area A to correct the results in the adjacent areas: thus, the maximum achievable accuracy level is that of area A. In case of MA-DSSE, instead, the second step estimation allows to integrate the information coming from all the adjacent areas with the local one. Thus, the estimation in area A is significantly improved, since the second step includes the useful voltage estimates of areas C and D (where the additional measurement points have been placed). In the same way, even the estimation in areas C and D are significantly refined. In case of area B, the enhancement is of course meaningful with respect to the LSE, even though it cannot reach the same level of the other areas because the voltage estimations of areas C and D cannot be involved in the second step.

The same considerations reported for the traditional measurements still hold for the case of synchronized measurements. The only difference concerns the phase-angle estimations. Again, also in this test, the phase-angle differences estimated with traditional measurements are really similar for all the estimators and close to the best estimation given by the ISE (with RMSEs lower than 1 mrad). The absolute phase angles computed in case of PMUs, instead, repeat the trend shown in Fig. 4 for the voltage magnitude estimation.

An additional test has been performed to confirm all the drawn conclusions. In this case, some other measurements have been deployed, simulating a future scenario with an improved measurement system. In particular, additional measurement points with respect to the previous test have been placed in nodes 25, 42, 48 (area B), and 91 (area C). Summarizing, in this augmented measurement system, four measurement points are present in area B, three in areas A and C, and two in area D.

Fig. 5 shows the results of the voltage magnitude estimation with traditional measurements. As it can be observed, area B provides the best local estimation as it has the larger number of voltage measurements. The MASE 1 method, as observed in the previous tests, allows the propagation of the best estimations in the close areas. Thus, area A acquires the better estimation coming from area B, and area D exploits that of area C. However, with the increased number of measurements, the enhancement coming from the use of the MA-DSSE is evident: the estimations are more accurate than MASE 1 method in all the areas and the improvement in the accuracy estimation is larger than in the previous tests. It is also interesting to note that the most accurate estimation for the MA-DSSE is obtained in area A, even if it does not have the largest number of measurements, since it can integrate the information coming from areas B, C, and D.

As aforementioned, when synchronized measurements are employed instead of traditional ones, similar results can be found. As an example, Fig. 6 reports the RMSE values of voltage magnitude estimations obtained using PMU measurements, under the same test conditions of Fig. 5. The RMSE profiles are very similar. The main differences are in the achievable accuracies, that in this case are, as can be expected, higher because of the lower uncertainties attributed to PMU measurements.

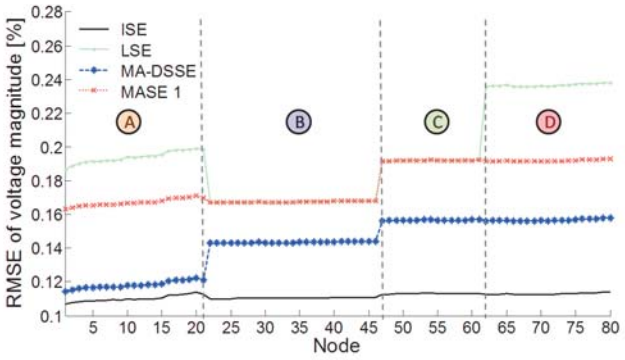

Fig. 5. RMSE of voltage magnitude estimation with augmented measurement system in case of traditional measurements

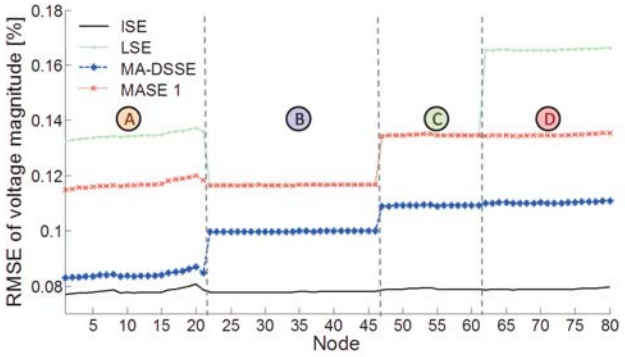

Fig. 6. RMSE of voltage magnitude estimation with augmented measurement system in case of PMU measurements

VI. Conclusions

In this paper a multi-area DSSE approach suitable for wide-area networks has been presented. The proposed method relies on the decomposition of the overall area in overlapping zones, with one shared node equipped with a measurement station. Such a solution allows the observability of each area, thus guaranteeing a reliable local estimation even in case of communication problems. The proposed multiarea architecture allows for a parallel operation of the local estimators, thus reducing the overall execution times. The estimation algorithm is composed of a two-step procedure where the first step local estimations are refined with a second step estimation that

exploits the estimates coming from the neighboring areas and suitably considers correlation in measurement process. A detailed description of the measurement model to be used in the estimation process has been presented. Performed tests confirm the feasibility and effectiveness of the proposed method.

APPENDIX A

In the following, the simplification of the mutual covariance matrix between two estimated state vectors of two adjoined areas is obtained. Substituting the area estimation matrices (11) into (14), it follows:

$$\boldsymbol{\Sigma}_{\mathbf{x}_A,\mathbf{x}_B} = \begin{bmatrix}\mathbf{B}_A & \mathbf{0}\end{bmatrix} \mathbf{W}_{TOT}^{-1} \begin{bmatrix}\mathbf{0} & \mathbf{B}_B\end{bmatrix}^{\mathrm{T}} \tag{17}$$

and, considering (12), it results:

$$\boldsymbol{\Sigma}_{\mathbf{x}_A,\mathbf{x}_B} = \begin{bmatrix}\boldsymbol{\Sigma}_A\mathbf{H}_A^{\mathrm{T}}\mathbf{W}_A & \mathbf{0}\end{bmatrix} \mathbf{W}_{TOT}^{-1} \begin{bmatrix}\mathbf{0} & \boldsymbol{\Sigma}_B\mathbf{H}_B^{\mathrm{T}}\mathbf{W}_B\end{bmatrix}^{\mathrm{T}} \tag{18}$$

Since the weighting matrix and the covariance matrix are symmetric, it is possible to rewrite the previous equation as follows:

$$\boldsymbol{\Sigma}_{\mathbf{x}_A,\mathbf{x}_B} = \begin{bmatrix}\boldsymbol{\Sigma}_A\mathbf{H}_A^{\mathrm{T}}\mathbf{W}_A & \mathbf{0}\end{bmatrix} \mathbf{W}_{TOT}^{-1} \begin{bmatrix}\mathbf{0} \\ \mathbf{W}_B\mathbf{H}_B\boldsymbol{\Sigma}_B\end{bmatrix} \tag{19}$$

In the Jacobians of the areas A and B indicated in (19), it is possible to separate the contributions of the measurements belonging only to a single area from those coming from the shared measurements:

$$\mathbf{H}_A = \begin{bmatrix}\mathbf{H}_{AA} \\ \mathbf{H}_{AB}\end{bmatrix}, \quad \mathbf{H}_B = \begin{bmatrix}\mathbf{H}_{BA} \\ \mathbf{H}_{BB}\end{bmatrix} \tag{20}$$

and, thus, it is possible to rewrite (19) as follows:

$$\begin{aligned}\boldsymbol{\Sigma}_{\mathbf{x}_A,\mathbf{x}_B} = &\begin{bmatrix}\boldsymbol{\Sigma}_A\mathbf{H}_{AA}^{T}\mathbf{W}_{AA} & \boldsymbol{\Sigma}_A\mathbf{H}_{AB}^{\mathrm{T}}\mathbf{W}_{AB} & \mathbf{0}\end{bmatrix} \times \\ &\times \begin{bmatrix}W_{AA} & \mathbf{0} & \mathbf{0} \\ \mathbf{0} & W_{AB} & \mathbf{0} \\ \mathbf{0} & \mathbf{0} & W_{BB}\end{bmatrix}^{-1} \times \begin{bmatrix}\mathbf{0} \\ \mathbf{W}_{AB}\mathbf{H}_{BA}\boldsymbol{\Sigma}_B \\ \mathbf{W}_{BB}\mathbf{H}_{BB}\boldsymbol{\Sigma}_B\end{bmatrix}\end{aligned} \tag{21}$$

Performing the matrix multiplication in (21), the covariance matrix can be finally expressed as follows:

$$\boldsymbol{\Sigma}_{\mathbf{x}_A,\mathbf{x}_B} = \boldsymbol{\Sigma}_A\mathbf{H}_{AB}^{\mathrm{T}}\mathbf{W}_{AB}\mathbf{H}_{BA}\boldsymbol{\Sigma}_B \tag{22}$$

APPENDIX B

In this Appendix the derivation of the covariance matrix between the estimates of two areas A and B is obtained for the case of synchronized phasor measurements. The rectangular coordinates formulation is used. In this case, there are two shared measurements between the areas for the common voltage measurement: the real part v_s^r and the imaginary part v_s^x. Thus, $\mathbf{H}_{AB}$ and $\mathbf{H}_{BA}$ in (15) (the rows of the two Jacobians corresponding to common measurements) become:

$$\mathbf{H}_{AB} = \mathbf{H}_{BA} = \begin{bmatrix}1,0,\ldots,0 \\ 0,1,\ldots,0\end{bmatrix} \tag{23}$$

Considering this, and considering that only the elements $\boldsymbol{\Sigma}_{\mathbf{x}_A,\mathbf{x}_B}(h,k)$ with $h = 1,2$ and $k = 1,2$ are needed, the following holds:

$$[\boldsymbol{\Sigma}_A\mathbf{H}_{AB}^{\mathrm{T}}] \Big|_{h=1,2} = \begin{bmatrix}\sigma^2_{v^r_{s_A}} & \sigma_{v^r_{s_A}v^x_{s_A}} \\ \sigma_{v^x_{s_A}v^r_{s_A}} & \sigma^2_{v^x_{s_A}}\end{bmatrix} \tag{24}$$

$$[\mathbf{H}_{BA}^{\mathrm{T}}\boldsymbol{\Sigma}_B] \Big|_{k=1,2} = \begin{bmatrix}\sigma^2_{v^r_{s_B}} & \sigma_{v^r_{s_B}v^x_{s_B}} \\ \sigma_{v^x_{s_B}V^r_{s_B}} & \sigma^2_{v^x_{s_B}}\end{bmatrix} \tag{25}$$

where the notation $\mathbf{P}|_{h=..;k=..}$ indicates the rows h or columns k to consider in the matrix $\mathbf{P}$, $\sigma_{v^r_{s_i}}$ and $\sigma_{v^x_{s_i}}$ (with $i = A, B$) are, respectively, the standard deviations of the real and imaginary voltage of the slack bus estimated by area i, and $\sigma_{v^r_{s_i}v^x_{s_i}}$ is the covariance. As for the weighting matrix, since PMUs provide the voltage phasor in polar coordinates, the derived rectangular coordinates have a full covariance matrix and its inverse $\mathbf{W}_{AB}$ is:

$$\mathbf{W}_{AB} = \begin{bmatrix}w_{v^r_s} & w_{v^r_sv^x_s} \\ w_{v^x_sv^r_s} & w_{v^x_s}\end{bmatrix} \tag{26}$$

Finally, the submatrix of interest of (15) becomes:

$$\begin{aligned}\boldsymbol{\Sigma}_{\mathbf{x}_A,\mathbf{x}_B} \Big|_{h=1,2;k=1,2} = &\begin{bmatrix}\sigma^2_{v^r_{s_A}} & \sigma_{v^r_{s_A}v^x_{s_A}} \\ \sigma_{v^x_{s_A}v^r_{s_A}} & \sigma^2_{v^x_{s_A}}\end{bmatrix} \times \\ &\begin{bmatrix}w_{v^r_s} & w_{v^r_sv^x_s} \\ w_{v^x_sv^r_s} & w_{v^x_s}\end{bmatrix} \times \begin{bmatrix}\sigma^2_{v^r_{s_B}} & \sigma_{v^r_{s_B}v^x_{s_B}} \\ \sigma_{v^x_{s_B}V^r_{s_B}} & \sigma^2_{v^x_{s_B}}\end{bmatrix} \\ = &\begin{bmatrix}\sigma_{v^r_{s_A}v^r_{s_B}} & \sigma_{v^r_{s_A}v^x_{s_B}} \\ \sigma_{v^x_{s_A}V^r_{s_B}} & \sigma_{v^x_{s_A}v^x_{s_B}}\end{bmatrix}\end{aligned} \tag{27}$$

where $\sigma_{v^r_{s_A}v^r_{s_B}}$ is the covariance between the real part of the voltage estimated in A and the real part of the voltage estimated in B and the other elements have analogous interpretations.

REFERENCES

[1] G. Celli, P. A. Pegoraro, F. Pilo, G. Pisano, and S. Sulis, "DMS cyber-physical simulation for assessing the impact of state estimation and communication media in smart grid operation," *IEEE Trans. Power Syst.*, vol. 29, no. 5, pp. 2436–2446, Sep. 2014.

[2] S. Chakrabarti, E. Kyriakides, and M. Albu, "Uncertainty in power system state variables obtained through synchronized measurements," *IEEE Trans. Instrum. Meas.*, vol. 58, no. 8, pp. 2452–2458, Aug. 2009.

[3] S. Chakrabarti, E. Kyriakides, G. Ledwich, and A. Ghosh, "Inclusion of PMU current phasor measurements in a power system state estimator," *Generation, Transmission & Distribution, IET*, vol. 4, no. 10, pp. 1104–1115, Oct. 2010.

[4] F. Aminifar, M. Shahidehpour, M. Fotuhi-Firuzabad, and S. Kamalinia, "Power system dynamic state estimation with synchronized phasor measurements," *IEEE Trans. Instrum. Meas.*, vol. 63, no. 2, pp. 352–363, Feb. 2014.

[5] M. E. Baran and A. W. Kelley, "State estimation for real-time monitoring of distribution systems," *IEEE Trans. Power Syst.*, vol. 9, no. 3, pp. 1601–1609, Aug. 1994.

[6] M. Baran and A. Kelley, "A branch-current-based state estimation method for distribution systems," *IEEE Trans. Power Syst.*, vol. 10, no. 1, pp. 483–491, Feb. 1995.

[7] W. M. Lin and J. H. Teng, "Distribution fast decoupled state estimation by measurement pairing," *Generation, Transmission and Distribution, IEE Proceedings-*, vol. 143, no. 1, pp. 43–48, 1996.

[8] H. Wang and N. Schulz, "A revised branch current-based distribution system state estimation algorithm and meter placement impact," *IEEE Trans. Power Syst.*, vol. 19, no. 1, pp. 207–213, Feb. 2004.

[9] M. Pau, P. A. Pegoraro, and S. Sulis, "Efficient branch-current-based distribution system state estimation including synchronized measurements," *IEEE Trans. Instrum. Meas.*, vol. 62, no. 9, pp. 2419–2429, Sep. 2013.

[10] M. Asprou, E. Kyriakides, and M. Albu, "The effect of variable weights in a WLS state estimator considering instrument transformer uncertainties," *IEEE Trans. Instrum. Meas.*, vol. 63, no. 6, pp. 1484–1495, Jun. 2014.

[11] C. Muscas, M. Pau, P. Pegoraro, and S. Sulis, "Effects of measurements and pseudomeasurements correlation in distribution system state estimation," *IEEE Trans. Instrum. Meas.*, 2014, in press. [Online]. Available: http://ieeexplore.ieee.org/stamp/stamp.jsp?tp=&arnumber=6814319
[12] A. Gomez-Exposito, A. de la Villa Jaen, C. Gomez-Quiles, P. Rosseaux, and T. Van Cutsem, "A taxonomy of multi-area state estimation methods," *Electric Power Systems Research*, vol. 81, no. 4, pp. 1060–1069, Apr. 2011.
[13] N. Nusrat, M. Irving, and G. Taylor, "Development of distributed state estimation methods to enable smart distribution management systems," in *Industrial Electronics (ISIE), 2011 IEEE International Symposium on*, Jun. 2011, pp. 1691–1696.
[14] L. De Alvaro Garcia and S. Grenard, "Scalable distribution state estimation approach for distribution management systems," in *Proc. 2nd IEEE PES Int. Conf. Exhibit. Innov. Smart Grid Technol. (ISGT Europe)*, Dec. 2011, pp. 1–6.
[15] C. Muscas, M. Pau, P. A. Pegoraro, S. Sulis, F. Ponci, and A. Monti, "Two-step procedures for wide-area distribution system state estimation," in *Proc. IEEE Int. Instrum. Meas. Technol. Conf. (I2MTC)*, May 2014, pp. 1517–1522.
[16] A. Abur and A. Gomez-Exposito, *Power System State Estimation. Theory and Implementation.* Marcel Dekker, New York, 2004.
[17] T. Van Cutsem, J. Horward, and M. Ribbens-Pavella, "A two-level static state estimator for electric power systems," *IEEE Trans. Power App. Syst.*, vol. PAS-100, no. 8, pp. 3722–3732, Aug. 1981.
[18] D. M. Falcao, F. F. Wu, and L. Murphy, "Parallel and distributed state estimation," *IEEE Trans. Power Syst.*, vol. 10, no. 2, pp. 724–730, May 1995.
[19] M. Zhao and A. Abur, "Multi area state estimation using synchronized phasor measurements," *IEEE Trans. Power Syst.*, vol. 20, no. 2, pp. 611–617, May 2005.
[20] A. Conejo, S. De La Torre, and M. Canas, "An optimization approach to multiarea state estimation," *IEEE Trans. Power Syst.*, vol. 22, no. 1, pp. 213–221, Feb. 2007.
[21] J. Zhu and A. Abur, "Effect of phasor measurements on the choice of reference bus for state estimation," in *Proc. IEEE Power Eng. Soc. General Meeting*, Jun. 2007, pp. 1–5.
[22] (2012) IEEE test feeder specifications. [Online]. Available: http://ewh.ieee.org/soc/pes/dsacom/testfeeders/

Carlo Muscas (M'98) received the M.S. (cum laude) degree in electrical engineering from the University of Cagliari, Cagliari, Italy, in 1994.

He was Assistant Professor with the University of Cagliari from 1996 to 2001. He has been an Associate Professor of Electrical and Electronic Measurement with the University of Cagliari, since 2001, where he is currently the Chairman of the Council for the M. S. degree in Electrical Engineering. He has authored or co-authored over 100 scientific papers. His current research interests include power quality phenomena, the measurement of synchronized phasors and the implementation of distributed measurement systems for modern electric grid. Mr. Muscas is currently an Associate Editor of the IEEE Transactions on Instrumentation and Measurement.

Marco Pau (S'14) received the M.S. degree in electrical engineering from the University of Cagliari, Cagliari, Italy in 2011, where he is currently pursuing the Ph.D. degree with the Department of Electrical and Electronic Engineering.

His current research interests include measurement systems applied to electric distribution grids and designed for distribution system state estimation.

Paolo Attilio Pegoraro (S'03-M'06) received the M.S. (cum laude) degree in telecommunications engineering and the Ph.D. degree in electronic and telecommunications engineering from the University of Padua, Padua, Italy, in 2001 and 2005, respectively. He currently holds a post-doctoral position with the University of Cagliari, Cagliari, Italy, where he focuses on the development of new measurement techniques for modern power networks. His current research interests include the measurement of synchronized phasors and the state estimation for electric distribution grids.

Sara Sulis (S'04, M'06) received the Ph.D. Degree in industrial engineering from the University of Cagliari, Cagliari, Italy, in 2006.

She is currently an Assistant Professor of Electrical and Electronic Measurements with the University of Cagliari. Her research activity concerns distributed measurement systems designed to study reliable methodologies to perform both state estimation and harmonic sources estimation of distribution networks. Her current research interests include power quality issues in power systems, with a special attention to harmonic pollution.

Ferdinanda Ponci (M'00, SM'08) received the M.S. and Ph.D. degrees in electrical engineering from the Politecnico di Milano, Milan, Italy, in 1998 and 2002, respectively.

She joined the Power and Energy Research Group with the Department of Electrical Engineering, University of South Carolina, Columbia, SC, USA, in 2003, as an Assistant Professor, where she was tenured and promoted Associate Professor in 2008. In 2009, she joined the Institute for Automation of Complex Power Systems with the E.ON Research Center, RWTH Aachen University, Aachen, Germany, where she is currently an APL Professor.

Antonello Monti (M'94, SM'02) received M.S. and Ph.D. degrees in electrical engineering from the Politecnico di Milano, Milan, Italy, in 1989 and 1994, respectively.

He was with the research laboratory, Ansaldo Industria, Milan, from 1990 to 1994. He joined the Department of Electrical Engineering with the Politecnico di Milano as an Assistant Professor. From 2000 to 2008, he was an Associate Professor and a Full Professor with the Department of Electrical Engineering, University of South Carolina, Columbia, SC, USA. He is currently the Director of the Institute for Automation of Complex Power Systems with the E.ON Energy Research Center, RWTH Aachen University, Aachen, Germany.